

Effect of Combustion Mode on Heat transfer inside a Hybrid Solar Receiver Combustor

A. Chinnici¹, Z.F. Tian¹, J.H. Lim¹, S. Long¹, G.J. Nathan¹, B.B. Dally¹

¹Centre for Energy Technology, School of Mechanical Engineering, The University of Adelaide, South Australia 5005, Australia

Abstract

A 3-D CFD model of a hybrid solar receiver combustor (HSRC) was developed to carry out a systematic assessment of multiple performance criteria (thermal efficiency and heat flux distribution) with the aim of identifying how the introduction of concentrated solar radiation inside the HSRC influences the relative performance of MILD and conventional combustion. The effect of changing the dominant receiver geometric features (i.e. the length-to-diameter cavity ratio) on the thermal performance of the device is also assessed. The model employs a Monte-Carlo ray tracing approach to calculate the radiation flux distribution on heat transfer fluid (HTF) pipes and thermal efficiency of the solar receiver under solar-only mode of operation. For the combustion-only mode of operation, two different burner designs were considered as representative cases for non-premixed swirl-stabilised flames and MILD combustion, respectively. It was found that through optimisation of the HSRC design it is possible to achieve similar thermal efficiency in both solar-only and combustion-only modes. Also, the thermal efficiency of the device increases with an increase in the length-to-diameter cavity ratio and solar concentration ratio. MILD and conventional combustion showed a similar thermal efficiency, although the total heat transfer rate was larger (up to 5%) under MILD conditions, implying a better utilisation of the energy source and/or fuel savings. On the other hand, the heat flux distribution on the HTF pipes for solar-only mode was closer to the combustion-only mode operating with conventional flames than MILD conditions, suggesting that the materials selection will be influenced by the combustion regime.

Introduction

Hybrids of concentrated solar thermal energy (CST) and combustion technologies are receiving growing attention due to the complementary nature of these two energy sources. The use of concentrated solar radiation (CSR) in power generation and process heat applications offers low net greenhouse gas emissions but suffers from high cost, due to the intermittent and variable nature of the resource, while the combustion of fossil fuels provides broad availability and low fuel cost, but at the expense of high CO₂ and pollutant emissions [1]. One opportunity to reduce the cost and increase the penetration of CST technology is to combine it with established technologies employing fossil fuels. Such hybrid systems can typically lower the cost of solar thermal power, due to the reduced infrastructure and potential thermodynamic synergies [2].

Recently, a novel concept of hybrid solar receiver combustor (HSRC) has been proposed [3, 4], in which the functions of a tubular solar receiver and a combustor are combined into a single device, which is used to harness both energy sources (solar and combustion). Previous studies [5-7] have shown that the HSRC offers advantages over existing hybrids (which collect the thermal

energy from the solar and combustion sources in separate devices and then combine them subsequently) of shared infrastructure and reduced start-up and shut down losses.

The HSRC design (Figure 1) allows the system to operate in three modes: solar-only (when solar radiation is abundant), combustion-only (in the absence of solar energy, with natural gas as the energy source) and a mixed-mode (a combination of both solar and combustion, to manage short and long term variability of the solar source). A HSRC device features a cavity, operable as a combustion chamber, with an aperture, to admit concentrated solar radiation into the chamber, multiple burners directly associated with the cavity to direct a flame into the device, and a heat transfer fluid (or a working fluid) heat exchanger within the cavity that receives heat energy from both energy sources (depending on the mode of operation). It also features a heat recovery system from the hot combustion products, whereby heat is circulated back into the HSRC and is used to preheat the combustion air. In one particular arrangement [8], the HSRC can be configured to operate with MILD combustion [9], as a mean to potentially enhance the performance of the device, owing to the intrinsic characteristics of this combustion regime [9].

All previous studies to date on the HSRC technology [5-8] employed an analytical model of mass and energy flows in the device, so that a detailed heat transfer analysis (involving flow field, chemistry, turbulence chemistry-interaction and solar ray-tracing) within the device is not yet available. To this end, the current study reports a detailed numerical comparative study of heat transfer (both convective and radiative) in MILD and conventional combustion (combustion-only mode) as well as under solar-only mode of operation with the aim to guide new understanding of the operating envelope.

Methodology

A 3-D CFD model of a hybrid solar receiver combustor (HSRC) was developed for both combustion-only and solar-only modes of operation. For the solar-only mode, the commercial software ANSYS/CFX 17 was employed. The Monte-Carlo ray tracing approach was used to model the concentrated solar radiation (CSR). The CSR flux entering the device was described with a Gaussian function (similar to a real heliostat field) [10], varying the peak flux in the range 1-5 MW/m². The focal point was located at the centre of the aperture plane and the number of rays was varied to achieve solution independence (the average number of rays tracked is ~2 million). The HSRC was positioned horizontally and the effect of buoyancy was included in the simulation (the effect of external wind was not considered in the present study). Mesh independence and mesh quality were checked to ensure the suitability of the mesh. In particular, the mesh quality was checked for skewness, aspect ratio, orthogonality and expansion factor. A total of approximately 2 million cells was employed for all configurations tested. For the combustion-only-mode, the

commercial software *ANSYS/FLUENT 17* was employed and two different burner designs [11, 12] were selected as representative cases for non-premixed swirl-stabilised flames and MILD regime. For these cases, only one quarter of the full domain was modelled and periodic boundaries were applied at the symmetry planes. For each case, four burners were considered with an inclination angle of 45°. The $k-\epsilon$ realizable model was selected as turbulence closure model. For the swirl-stabilised flame configuration, the eddy-dissipation with a global (2-steps) kinetic mechanism was employed while for the MILD regime, the eddy-dissipation concept with a 4-step mechanism was used. Methane was considered as fuel. A mesh of ~ 3.5 million cells was employed for the combustion-only cases. The DO method was selected to describe the radiative equation and the weighted-sum-of-gray gases model (WSGGM) was used to calculate the spectral properties. The convergence criterion for all cases was set to be 1×10^{-6} . For both modes of operation, the total power input was fixed at 250 kW. The boundary conditions of the CFD model (mass flow rates and temperature of air and fuel jets and temperature of receiver pipes) were obtained employing an analytical model of the HSRC, developed previously [5-8]. The walls of the HSRC were considered adiabatic for all the cases analysed while the external heat exchanger was not considered in the domain investigated. The flow of the heat transfer fluid, HTF, within the receiver pipes was not modeled and a fixed temperature was applied on the outer diameter of the HTF pipes. The key geometrical features of the HSRC configurations investigated and the operative conditions considered are reported in Tables 1 and 2.

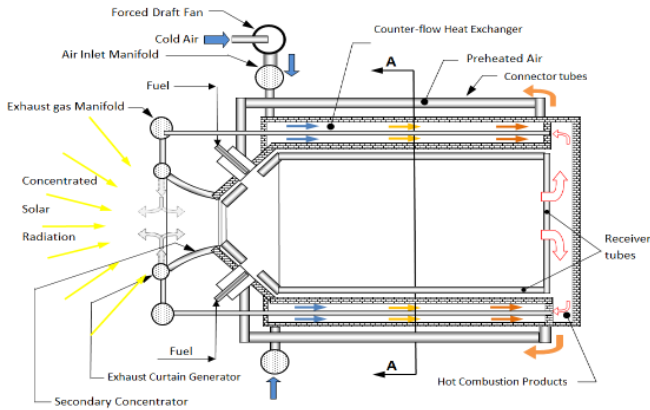


Figure 1. Configuration of the Hybrid Solar Receiver Combustor.

Case	L/D	D, mm	# Pipes
HSRC-SWIRLBURNER	3-5-7	400	36
HSRC-MILDBURNER	3-5-7	400	36

Table 1. Key geometrical features of the device, for all the cases investigated.

L/D	Fuel Input, kW	Air Input, kW	T _{fuel} , K	T _{air} , K
3	211	39	300	765
5	208	42	300	805
7	207	43	300	820

Table 2. Operative working conditions (combustion-only), for all the cases investigated.

Results and Discussion

Figure 2 presents the deduced flow-patterns and the temperature field within the HSRC under combustion-only, for both MILD and

conventional combustion configurations ($L/D = 5$). For the MILD case, the flow-field features two distinct recirculation zones, which are generated by the interaction of the high-momentum inlet air jets (after impinging on each other). The strong internal recirculation of the hot products within the device facilitates the establishment of MILD regime. The thermal field at the centreline plane highlights a quasi-homogeneous temperature distribution within the main cavity, typical of the MILD combustion regime. For the HSRC operating with conventional combustion, close to the burner exit, the flow-field features the well-known central recirculation zone (CRZ). In addition to the CRZ, the use of multiple swirl burners also generates a large low-swirl (low-velocity) structure, which extends for the entire cavity.

Figure 3 shows the thermal efficiency, η_{th} , as a function of the length-to-diameter ratio, L/D , for all the cases investigated under combustion-only mode of operation. The calculated η_{th} employing the analytical model developed by Lim et al. (2016) and those obtained under solar-only mode of operation ($F_{peak} = 1$ and 2 MW/m^2) are also shown for comparison. For the solar-only mode, η_{th} was defined as $\frac{\dot{Q}_{useful}}{\dot{Q}_{solar,in}}$ where $\dot{Q}_{solar,in}$ is the amount of the total power coming from the concentrator intercepted by the aperture.

For the combustion-only mode, $\eta_{th} = \frac{\dot{Q}_{useful}}{\dot{Q}_{fuel,in}}$, where $\dot{Q}_{fuel,in}$ is the total fuel input (Table 1). It can be seen that L/D influences significantly the thermal performance of the device under combustion-only mode of operation. In particular, an increase of L/D leads to an increase in η_{th} . It can also be seen that the analytical model [5] predicts a larger η_{th} (up to 52% difference, for short cavities) and a different slope of the η_{th} -curve in comparison with the present study. However, a good agreement was found for long cavities, suggesting that the use of the analytical model [5] to predict the thermal performance of the device should be limited to long cavities. The MILD case (HSRC-MILDBURNER configuration) shows a larger η_{th} in comparison with the conventional combustion case, implying a better utilisation of the energy source. Figure 3 also shows that the device can achieve similar performance under either solar-only or combustion-only, depending on the solar peak flux, although η_{th} is lower under the combustion-only mode of operation. This suggests that the heat transfer rate under solar-only mode is more efficient. This is mainly attributed to the different heat transfer mechanisms, i.e. purely by a radiative heat transfer under solar-only and due to a combined radiative and convective heat transfer under combustion-only mode (as shown in Figure 4). Figure 4 also highlights that the enhanced η_{th} calculated for the selected configurations for the MILD regime in comparison with conventional combustion is mainly due to a larger convective heat transfer.

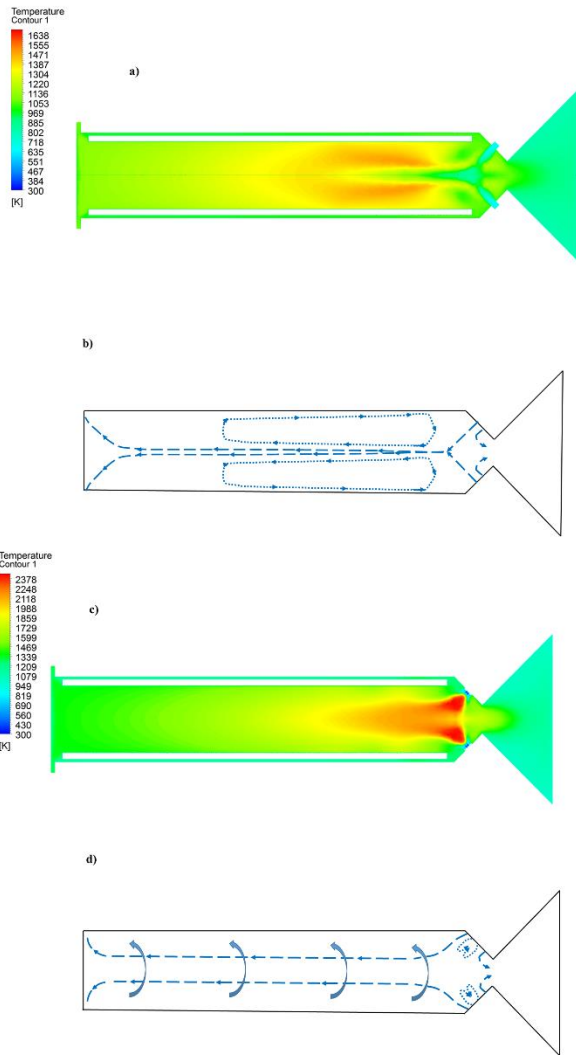


Figure 2. Deduced flow-patterns (b and d) and thermal fields (a and c) within the HSRC for the MILD (a and b) and conventional combustion (c and d) cases ($L/D = 5$).

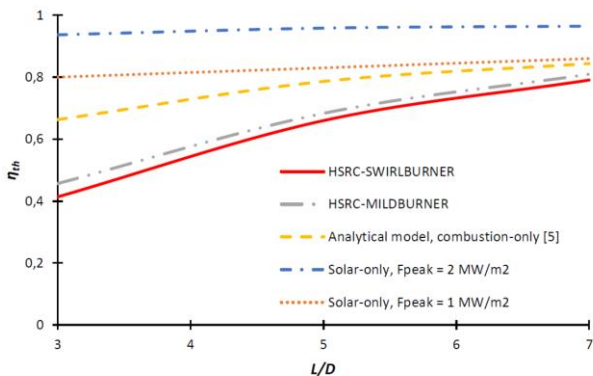


Figure 3. Calculated thermal efficiency under combustion-only (MILD and conventional flame) and solar-only ($F_{peak} = 1$ and 2 MW/m^2) as a function of L/D . Also reported, is η_{th} calculated employing the analytical model [5].

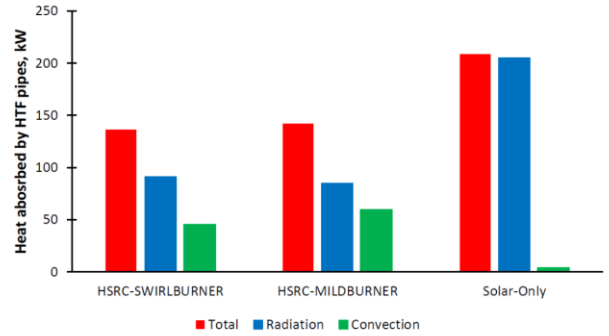


Figure 4. Calculated total, radiative and convective heat absorbed by the HTF pipes, under combustion-only (MILD and conventional flame) and solar-only ($F_{peak} = 1 \text{ MW/m}^2$), for $L/D = 5$.

Figure 5 presents the average heat flux distribution on the HTF pipes for all the case considered ($L/D = 5$). The calculated heat flux distribution obtained for solar-only mode of operation ($F_{peak} = 4 \text{ MW/m}^2$) is also shown for comparison. It can be seen that a uniform heat flux distribution, typical of the MILD regime, features the HSRC-MILDBURNER case. Figure 5 also shows that the calculated heat flux distribution on the receiver tubes under solar-only mode and MILD regime are significantly different, implying different thermal stresses on the HTF pipes. This suggests that the use of special materials (higher resistance to thermal shocks) would be required for the MILD HSRC compared to the HSRC employing conventional combustion (HSRC-SWIRLBURNER).

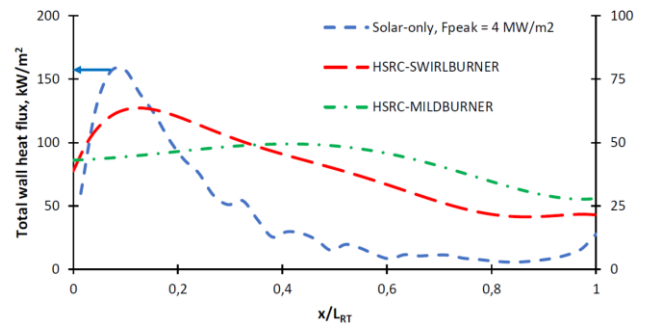


Figure 5. Calculated average heat flux distribution on HTF pipes, under combustion-only (MILD and conventional flame) and solar-only ($F_{peak} = 4 \text{ MW/m}^2$), for $L/D = 5$.

Conclusions

The key outcomes from the numerical investigation of the thermal performance in a HSRC under solar-only and combustion-only modes of operation are as follows:

- The thermal performance of the device increases significantly with an increase in L/D ratio (combustion-only) and solar peak flux (solar-only mode);
- The device can achieve similar performance under the two different modes of operation;
- The radiative transfer is the dominant heat transfer mechanism under solar-only mode. Under combustion-only, the heat transfer is due to a combination of radiation and convection;
- The use of MILD combustion leads to a larger η_{th} in comparison with non-premixed swirled flames;
- Swirl-stabilised flames and solar-only mode show a similar heat flux distribution on HTF pipes in comparison with that obtained with MILD regime. This implying that the materials will undergo to similar

stresses under the two different modes of operation if a swirl-stabilised flame is selected (i.e. no special materials are required, with beneficial effects on the overall costs).

Acknowledgments

The support of the Australian Research Council and of FCT Combustion and Vast Solar through the ARC Linkage scheme is gratefully acknowledged.

References

- [1] Kreith, F., Goswami, D.Y. (2007). Handbook of Energy Management and End Use Efficiency, CRC Press.
- [2] Peterseim, J.H., et al. (2013). Concentrated solar power hybrid plants, which technologies are best suited for hybridisation? *Renewable Energy*, 57: 520-532.
- [3] Nathan, G.J., et al. (2013). A hybrid receiver-combustor. US Patent 2015/0054284, A.R.I.P. Ltd, Editor.
- [4] Nathan, G.J., et al. (2014). Economic evaluation of a novel fuel-saver hybrid combining a solar receiver with a combustor for a solar power tower. *Applied Energy*, 113: 1235-1243.
- [5] Lim, J.H., et al. (2016). Analytical assessment of a novel hybrid solar tubular receiver and combustor. *Applied Energy*, 162: 298-307.
- [6] Lim, J.H., et al. (2016). Impact of start-up and shut-down losses on the economic benefit of an integrated hybrid solar cavity receiver and combustor. *Applied Energy*, 164: 10-20.
- [7] Lim, J.H., et al. (2016). Techno-economic assessment of a hybrid solar receiver and combustor. *AIP Conference Proceedings*, 1734: 070020.
- [8] Lim, J.H., et al. (2016). Development of a Hybrid Solar Receiver Combustor Operating with Mild Combustion. *Energy*, under review.
- [9] Cavaliere, A., and de Joannon, M. (2004). MILD Combustion. *Progress in Energy and Combustion Science*, 30: 329-366.
- [10] Steinfeld et al. (1993). Optimum aperture size and operating temperature of a solar cavity-receiver. *Solar Energy*, 50:19-25.
- [11] Weber, R., et al. (2000). On the (MILD) combustion of gaseous, liquid, and solid fuels in high temperature preheated air. *Proceedings of the Combustion Institute*, 28: 1315-1321.
- [12] Meier, W., et al. (2000). Investigations in the TECFLAM swirling diffusion flame: Laser Raman measurements and CFD calculations. *Applied Physics B*, 71: 725-731.